[23] G. Felic and E. Skafidas, "Flip-chip interconnection effects on 60 GHz microstrip antenna performance," *IEEE Antennas Wireless Propag. Lett.*, vol. 8, pp. 283–286, May 2009.
[24] S. T. Choi, K. S. Yang, K. Tokuda, and Y. H. Kim, "60 GHz transceiver module with coplanar ribbon bonded planar millimeter-wave bandpass filter," *Microw. Opt. Technol. Lett.*, vol. 49, no. 5, pp. 1212–1214, 2007.
[25] Y. Sun, S. Glisic, F. Herzel, K. Schmalz, E. Grass, W. Winkler, and R. Kraemer, "An integrated 60 GHz transceiver front end for OFDM in SiGe: BiCMOS," presented at the Wireless World Research Forum 16, Shanghai, China, Apr. 26–28, 2006.
[26] [Online]. Available: http://www.hittite.com/content/documents/data_sheet/hmc-alh382.pdf

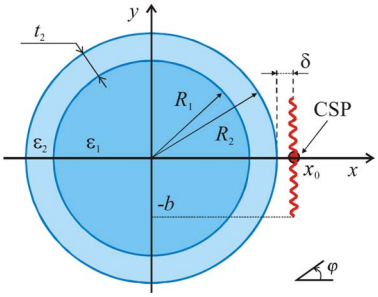

Fig. 1. Geometry and notations of the problem. The curve line indicates the branch cut in real space due to CSP oriented to radiate at $\varphi = 180°$.

Two-Shell Radially Symmetric Dielectric Lenses as Low-Cost Analogs of the Luneburg Lens

A. V. Boriskin, A. Vorobyov, and R. Sauleau

***Abstract*—This communication provides guidelines for the design of two-shell radially symmetric dielectric lenses with collimating capabilities compatible with those of the classical Luneburg lens. Unlike earlier publications, it is demonstrated that such a lens can be designed using any standard low permittivity dielectric materials, provided the optimal shell thickness is selected. The lens characteristics are studied in 2-D formulation using exact series representation. A detailed description is given for lenses with radius of 10 λ_0 and core made of Rexolite. The design recommendations are then generalized for lenses with radii of 5 to 15 λ_0 and cores made of Teflon, Fused Silica and Quartz. Finally, a chart defining the optimal shell thickness for lenses made of two arbitrary dielectric materials is provided. Validity of the recommendations for design of 2-D and 3-D radially symmetric lenses is proven by comparison with optimal designs reported by other authors.**

***Index Terms*—Dielectric lens, lens antennas, luneburg lens.**

I. Introduction

A radially symmetric dielectric lens capable of collecting rays in a focus on its rear surface is an attractive solution for many applications from microwave to optical ranges [1]–[10]. Such a lens, known as the Luneburg lens (LL) [11], can be designed as a radially inhomogeneous or multi-shell sphere, e.g., [2], [5], [12]. A critical aspect in the design of multi-shell LLs is the limited number of available low-loss dielectric materials whose permittivity belongs to the range of 1–2, as suggested by the ray-optics focusing rule

$$\varepsilon(r) = 2 - \left(\frac{r}{R}\right)^2, \quad r \in [0, R] \tag{1}$$

Manuscript received September 20, 2010; revised November 14, 2010; accepted December 13, 2010. Date of publication June 07, 2011; date of current version August 03, 2011. This work was supported in part by the Université Européenne de Bretagne, France, by the ESF in the framework of the RNP-NEW-FOCUS, by the Fondation Michel Métivier, and in part by the North Atlantic Treaty Organization under Grant RIG983313.

A.V. Boriskin is with the Institute of Radiophysics and Electronics NASU, Kharkov, Ukraine, and also with the Institute of Electronics and Telecommunications of Rennes (IETR), UMR CNRS 6164, University of Rennes 1, Rennes, France (e-mail: artem.boriskin@ieee.org).

A. Vorobyov and R. Sauleau are with the Institute of Electronics and Telecommunications of Rennes (IETR), UMR CNRS 6164, University of Rennes 1, Rennes, France.

Color versions of one or more of the figures in this communication are available online at http://ieeexplore.ieee.org.

Digital Object Identifier 10.1109/TAP.2011.2158793

where R is the lens radius, or its discrete analog for the uniformly-layered LL

$$\varepsilon_n = 2 - \left(\frac{(n-0.5)}{N}\right)^2, \quad n = 1, \ldots, N \tag{2}$$

where ε_n is permittivity of the n-th layer and N is the total number of layers ($n = 1$ corresponds to the most inner layer).

There are well known ways to fabricate artificial materials with desired properties via milling holes or adding compounding materials, e.g., [13]–[15]. Nevertheless each of them increases complexity and cost of the technology especially for multi-shell lenses. Therefore a favorable solution for low-cost radially symmetric lenses is a single- or double-shell design with layers made of the available low-loss dielectric materials, e.g., [1], [3], [4], [6], [12].

As demonstrated in [12], the minimum number of layers needed to provide the collimating capabilities compatible to those of a classical LL is two. The optimal design for the two-shell lens, found in [12] using global optimization technique, is a dense quartz-like core covered with a quarter-wavelength matching layer. Such a design exhibits critical drawbacks, namely: increased overall weight, difficulties in fabrication and further exploitation of a fragile matching layer, and finally involvement of the whispering gallery (WG) modes whose impact on the antenna characteristics grows rapidly with increase of the dielectric contrast on the shell boundaries [16].

In this communication we demonstrate that a two-shell lens with desired collimating capabilities can be designed using any standard low permittivity dielectric materials. We also present a chart with tabulated data generated from many simulation cycles that enables one to determine the optimal parameters of a two-shell lens made of two arbitrary dielectric materials without solving the corresponding diffraction problem.

The communication is built as follows. After a brief outline of the solution given in Section II, a Rexolite-core lens illuminated by a wave beam is studied in detail in Section III-A. Then the impacts of the lens size, feed location and core material are investigated in Sections III-B–III-D, respectively. Finally, conclusions are outlined in Section IV.

II. Outline of the Solution

We consider the problem in two-dimensional (2-D) formulation and model the lens as a multi-shell circular dielectric cylinder (Fig. 1). To study its collimating capabilities, the lens is illuminated by a wave beam radiated by a complex-source point (CSP) feed, i.e., a line current located in a point with a complex coordinate. In real space such a feed radiates a beam whose waist is controlled by the value of the imaginary part of its coordinate, b [17].

We solve the problem using in-house software based on the exact series representation [16]. The software is capable of fast and accurate characterization of 2-D multi-shell circular lenses with full account of optical and modal features intrinsic to finite-size lenses and effects related to the directive nature of the primary feed. In particular, our software enables us to accurately account for the WG resonances, which is a bottleneck for most of conventional techniques [18], [19].

The radiation characteristic considered here as a measure of the lens collimating capability is the broadside directivity of the CSP feed assisted by the lens defined as $D = 2\pi|U(\varphi_m)|^2/P_{tot}$, where U is the E_z or H_z field component (for the case of E or H polarization, respectively), $\varphi_m = 180^\circ$ is the broadside direction, and P_{tot} is the total radiated power integrated over all directions. Finally, the aperture efficiency of a 2-D antenna is defined as $\eta_a = D\,\lambda_0/4\pi R$.

As a reference solution we consider two-shell and seven-shell lenses designed in accordance with (2). Note that the latter (seven-shell LL) is recognized as a good staircase approximation of the conventional inhomogeneous LL [16].

III. Numerical Results

For numerical analysis we consider lenses of three different sizes ($R_2 = 5\ \lambda_0$, $10\ \lambda_0$, and $15\ \lambda_0$) with cores made of standard low permittivity materials, such as Teflon ($\epsilon = 2.1$), Rexolite ($\epsilon = 2.53$), Fused Silica ($\epsilon = 3.27$), and Quartz ($\epsilon = 3.8$), e.g., [3], [6], [7], [20]. The outer shells are assumed to be made of arbitrary dielectric materials whose permittivity is below the one of the core material. As possible candidates for the outer shell, Polyurethane foam (PUF, $\epsilon = 1.2$) [14] and Teflon are considered. All materials are assumed to be isotropic and lossless. The lens radii are given in terms of wavelengths in free space (λ_0), so the results are applicable to any frequency range, provided the proper permittivity value is considered.

In simulations, unless certain values are indicated, the CSP feed is located at a fixed distance from the lens surface ($\delta = \lambda_0/10$), and its beam waist parameter kb equals 3.0 ($k = 2\pi/\lambda_0$ is a free space wavenumber) that corresponds to the full half-power beamwidth of 36°. This value is selected as the average best for all the considered two-shell lenses (see Appendix).

A. Two-Shell Lens With a Core Made of Rexolite

The design of a two-shell lens is determined by four parameters, namely: radii and permittivity of both shells. If the core material and the outer shell radius are fixed, it is possible to plot a contour graph describing the lens collimating capability versus two other parameters, i.e., permittivity and thickness of the outer shell. For the sake of generalization, it is convenient to replace the outer shell thickness by a normalized parameter, namely the ratio between inner and outer radii. As it will be demonstrated, the optimal radii ratio is almost frequency independent.

Fig. 2 shows the broadside directivity of the E- and H-polarized CSP feeds assisted by two-shell Rexolite-core lenses with $R_2 = 10\ \lambda_0$. As one can see, to achieve the best directivity a proper ratio between the shells radii and permittivity should be provided. Moreover, there exists a wide range of parameters providing the directivity close to its maximum value (see the white contour line); this gives a freedom in selecting parameters of the outer shell that suit the formulated optimal performance condition (1 dB degradation of directivity from its maximum value). For instance, if one wishes to design the outer shell in PUF or Teflon, the proper ratio of the shells radii is 0.83 and 0.56, respectively (see marks in Fig. 2), whereas the best performance would be achieved for $\epsilon_2 = 1.6$ and $R_1/R_2 = 0.72$. The aperture efficiency of these designs equals 62%, 56%, and 66%, respectively. As shown in Sections III-B and III-C, the optimal radii ratio may require correction depending on the lens size and feed position.

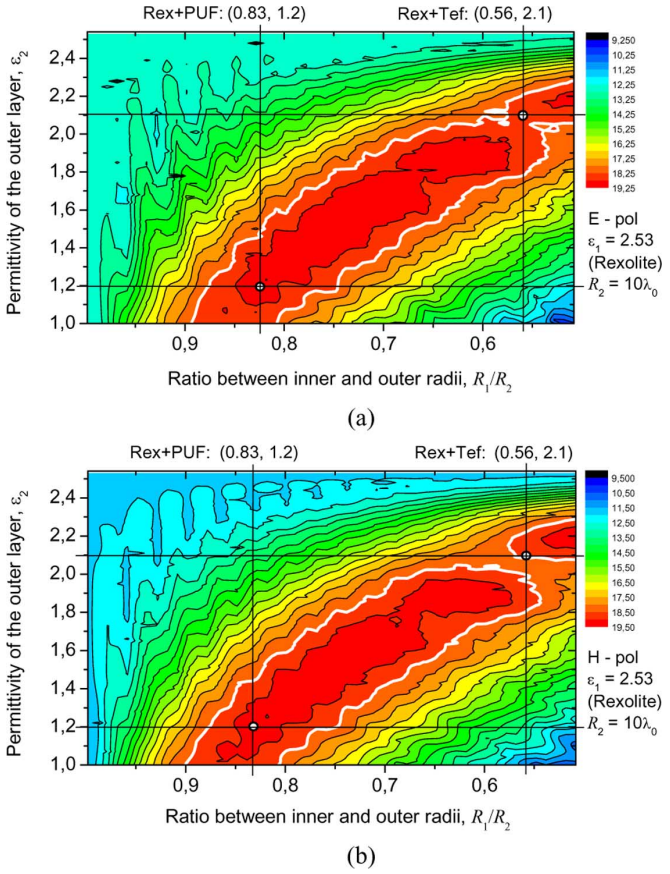

Fig. 2. Color map representing the broadside directivity of the CSP feed assisted by a two-shell Rexolite-core lens ($R_2 = 10\ \lambda_0$) versus the ratio between the inner and outer shells radii and the outer shell permittivity: (a) E-polarization, (b) H-polarization. The white contour line corresponds to the 1 dB degradation level with respect to the maximum value of the directivity (see the color bar for the scale).

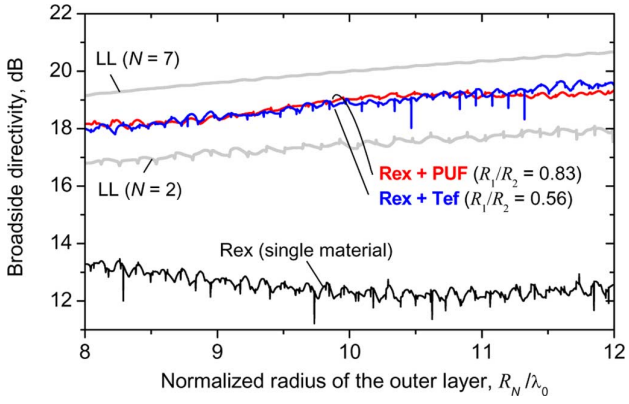

Fig. 3. Broadside directivity of the CSP feed assisted by the uniformly-layered LLs (made of two and seven layers) and their low-cost analogs, i.e., a single-material lens and optimized two-shell lenses with cores made of Rexolite and outer shells made of PUF and Teflon, respectively. Parameters of the optimized two-shell lenses correspond to the marks in Fig. 2.

Comparison between Fig. 2(a) and (b) shows that performance of the lens is almost polarization insensitive. This is also confirmed by comparing the radiation patterns computed for the selected lens configurations: they reveal identical side lobes down to -20 dB (skipped for brevity). Because of this we limit further discussion by the E-polarization case only.

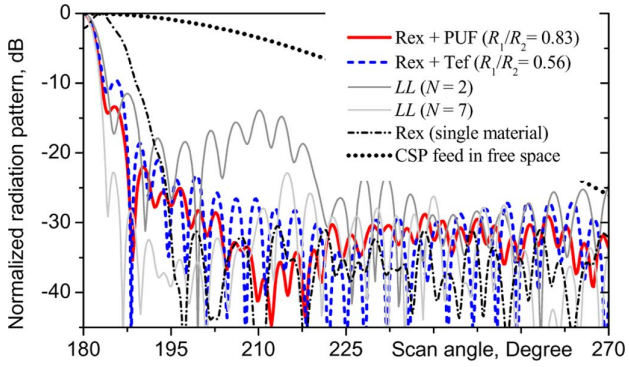

Fig. 4. Normalized radiation patterns produced by the lenses whose performance is studied in Fig. 3. The lenses have the same size $R_N = 10\ \lambda_0$.

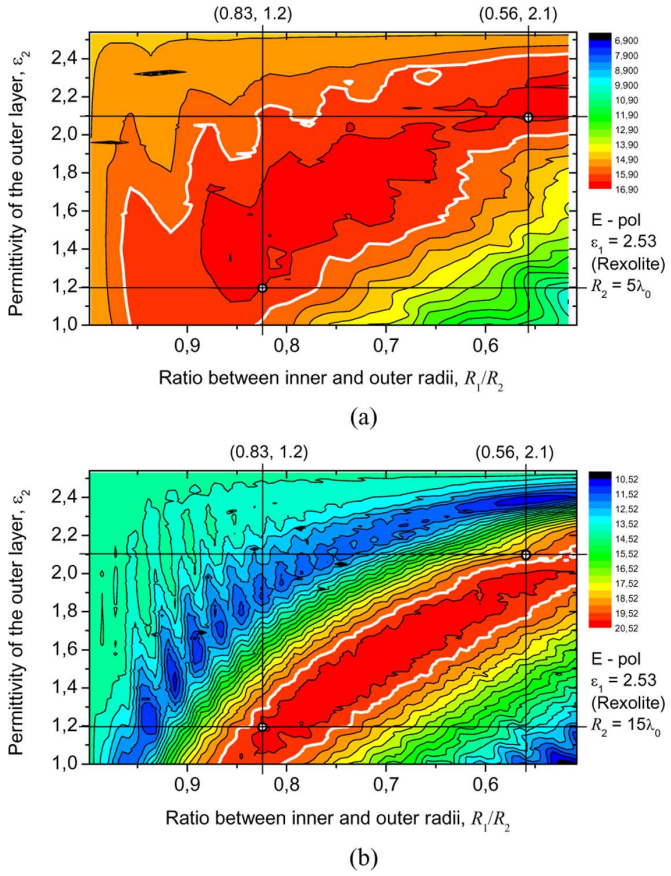

Fig. 5. Same as Fig. 2(a) for lenses of different sizes: (a) $R_2 = 5\ \lambda_0$, (b) $R_2 = 15\ \lambda_0$. The reference marks are the same as in Fig. 2.

In Fig. 3 the broadside directivity of the optimized two-shell lenses (Rex + PUF and Rex + Tef) is shown in the frequency range of $\pm 20\%$ from the central value of the frequency parameter. Their performance is superimposed with that of a single-material Rexolite lens and two reference LLs made of two and seven shells, whose parameters are defined in accordance with (2). As it is seen, the optimized two-shell lenses significantly outperform a single-material lens and are almost as good as the seven-shell LL. The advanced performance is preserved over the whole frequency range.

It is interesting to note the presence of sharp periodic spikes (associated with WG resonances [16]) observed for the single-shell and two-shell (Rex + Tef) lenses in Fig. 3. As one can see, for lenses with contrast boundaries directivity degradation due to WG modes can exceed 20% (e.g., about 1 dB for the single-material Rexolite lens). For

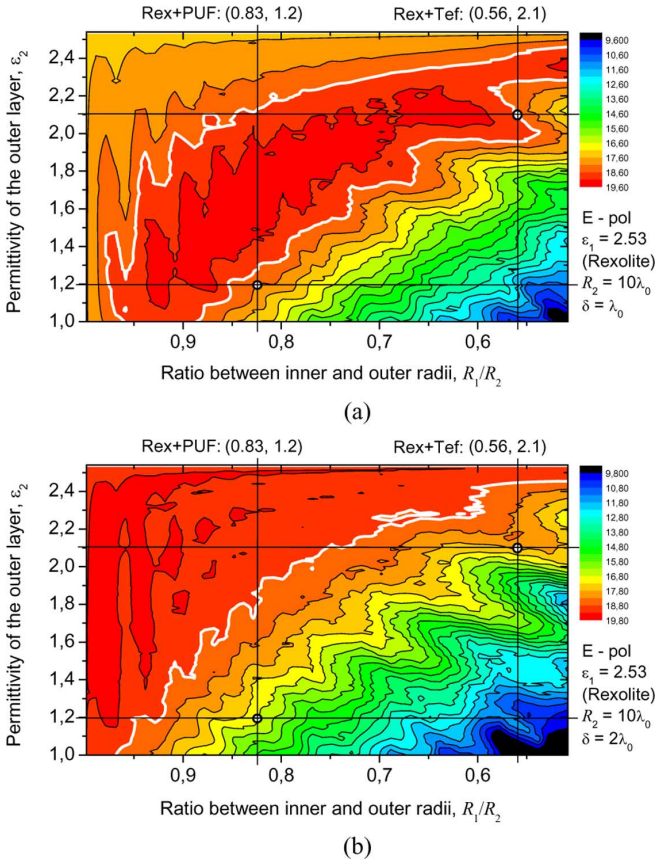

Fig. 6. Same as Fig. 2(a) for the CSP feed placed at a certain distance from the lens surface: (a) $\delta = \lambda_0$, (b) $\delta = 2\ \lambda_0$. The marks are the same as in Fig. 2.

realistic antennas, the impact of WG resonances is usually less pronounced due to dissipation losses, non-ideal spherical shape of the lens, presence of lens supports and a matched feed, etc. Nevertheless, one has to note that WG resonances can exist not only at the lens periphery but also at the inner shells boundaries (out of reach of the lens supports and feed). Thus they can also affect the performance of multi-shell lenses, especially those with air gaps and dense cores [21].

The far-field patterns produced by the selected lenses are shown in Fig. 4. As seen, the optimized two-shell Rexolite-core lenses produce a main beam with the same half-power beamwidth as the seven-shell LL, which is twice narrower than observed for the single-material lens. They also suppress side lobes down to -20 dB (except the first side-lode) that is ~ 5 dB better than observed for the two-shell LL.

B. Impact of the Lens Size

Fig. 5 represents the broadside directivity of the Rexolite-core lenses with radius of 5 λ_0 and 15 λ_0. Compared to similar graphs shown in Fig. 2 for the lens with $R_2 = 10\ \lambda_0$, the optimal radii ratio slightly shifts towards larger values when lens size reduces and vice versa when lens size grows (note the reference marks in Figs. 2 and 5). Moreover, the area of the optimal parameters combinations (denoted by a white contour line) becomes more narrow and less indented. The former is a corollary of the growing size of the lens, whereas the latter is due to the reduced impact of internal reflections on the performance of a larger size lens.

C. Impact of the Feed Location

Fig. 6 demonstrates the impact of the feed location on the optimal configuration of the lens. As one can see, the farther the feed from the lens

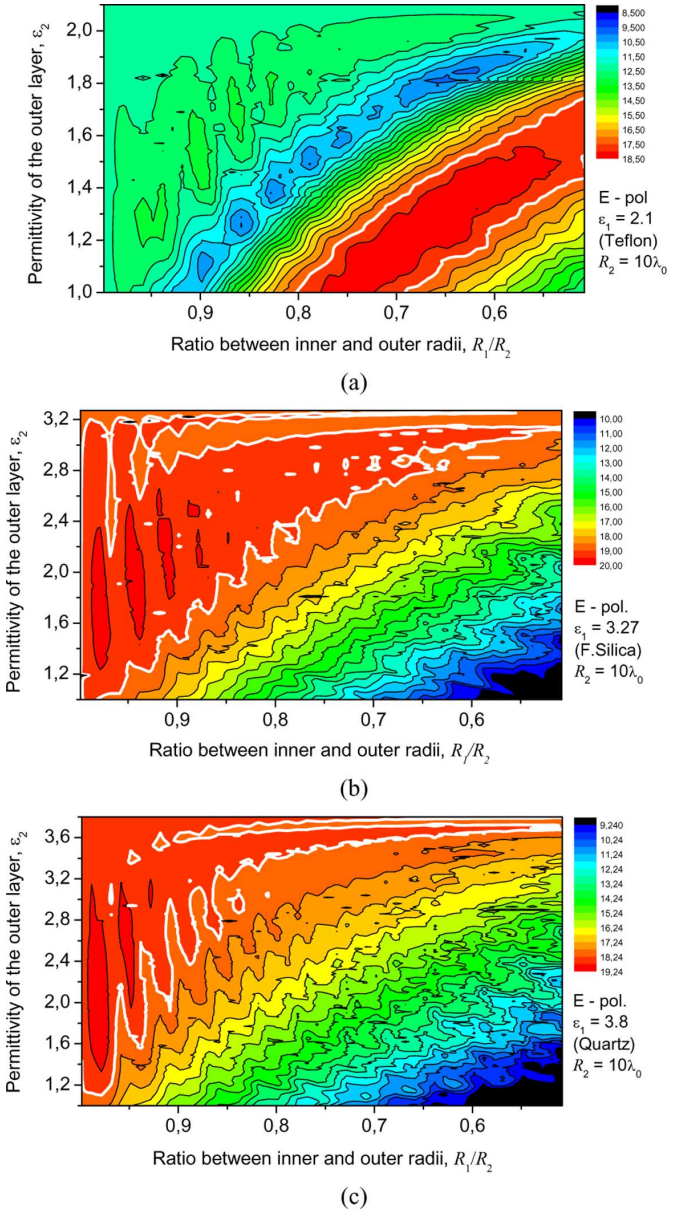

Fig. 7. Same as Fig. 2(a) for the lenses ($R_2 = 10\ \lambda_0$) with cores made of: (a) Teflon, (b) Fused Silica, and (c) Quartz.

surface, the larger core is needed to effectively collimate the beam. As the optimal core size grows proportionally to the increase of the δ parameter, a corresponding correction factor can be introduced, if necessary. A detailed description of the feed position influence on the lens antenna performance is available in [1], [3] and thus it is not discussed here.

D. Impact of the Lens Material

As one can see in Fig. 7 (to be considered together with Fig. 2), the higher the permittivity of the core material, the larger the relative size of the core required to provide the optimal performance of the lens. In fact, a single-shell lens made of a quartz-like material (with $\varepsilon \geq 3.2$) is already capable of providing directivity value close to the best one of the two-shell Rexolite-core lens, although it can suffer from high back-reflection and WG resonances. To obtain the best performance with such lenses a thin matching layer is required (which is in line with conclusions of [12]). What is new comparing to the earlier studies is the demonstrated possibility of designing lenses with favorable collimating capabilities using any two low-permittivity materials (see Figs. 2 and 7).

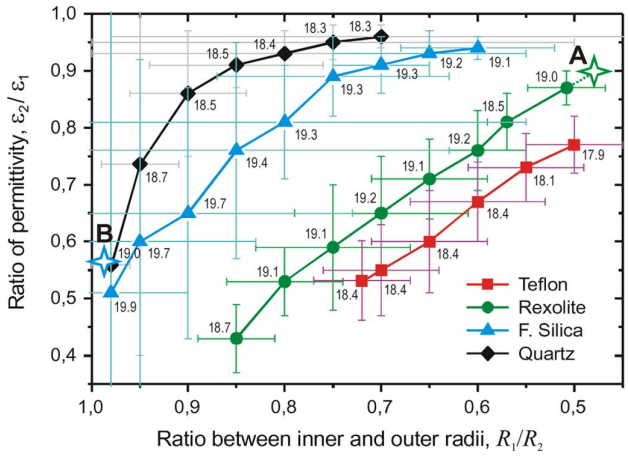

Fig. 8. Cumulative chart representing the optimal pairs of relative parameters (radii and permittivity) for lenses with $R_2 = 10\ \lambda_0$ and cores made of different materials (see legend). The corresponding directivity values are shown nearby. The error bars indicate the range of parameters that guarantees deviation of the directivity value from its peak value for not more than 1 dB (see white contour lines in Figs. 2 and 7). The star marks indicate optimal designs reported in [6], [7] and [12], namely: (A) Rexolite-Polyethylene ($\epsilon_2 = 2.25$) lens with $R_1/R_2 = 0.47$ and (B) synthesized two-shell lens made of two arbitrary materials ($\epsilon_1 = 3.29, \epsilon_2 = 1.87$) with $R_1/R_2 = 0.98$. The color of stars corresponds to the core material permittivity value.

To give a hint on how to select the optimal parameters of a two-shell lens, a chart summarizing findings for lenses studied in Figs. 2 and 7 is plotted in Fig. 8. Here, each mark indicates a pair of the optimal parameters (i.e., ratio of radii and permittivity of inner and outer shells) for lenses with cores made of the selected materials (see legend). The error bars associated with each mark show the flexibility in selecting the parameters in order to keep within the 1 dB range from the peak directivity. As it is seen, the increase of the core material permittivity continuously shifts the curve towards higher R_1/R_2 values and bends it towards the higher $\varepsilon_2/\varepsilon_1$ values. This regularity enables one to predict the optimal parameters of a two-shell lens made of arbitrary dielectric materials by interpolating the available data. Note that additional correction is required depending on the lens size and feed position (see Sections III-B and III-C).

IV. Conclusion

It is demonstrated that two-shell radially symmetric lenses with collimating capabilities compatible with that of the conventional uniformly-layered multi-shell LL can be designed using standard low permittivity dielectric materials. The key to success is shown to be a proper selection of the shells thickness. The numerical data, computed for lenses of different size and material, have been collected and organized in a chart enabling one to determine the optimal parameters of a two-shell lens made of two arbitrary dielectric materials without solving the corresponding diffraction problem. The validity of the outlined recommendations for design of 2D and 3D lenses is proven by the excellent agreement with experimental and numerical data reported in earlier publications.

Appendix
Optimal Illumination Conditions for Multi-Shell and Two-Shell Lenses

Fig. 9 represents the broadside directivity of the CSP feed assisted by a seven-shell LL whose parameters are defined in accordance with

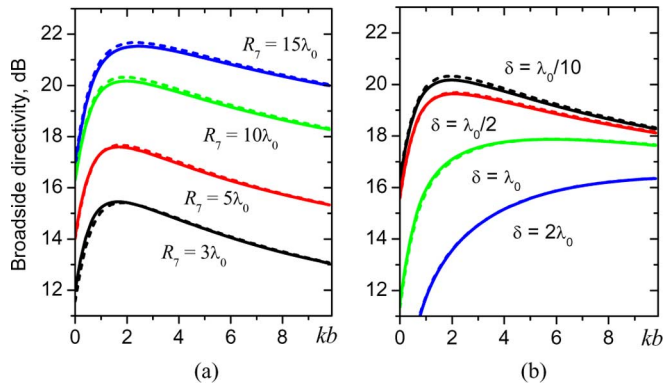

Fig. 9. Broadside directivity of the CSP feed assisted by a uniformly-layered seven-shell LL vs. beam waist parameter: (a) lenses of different size with feed located close to the lens surface $\delta = \lambda_0/10$, (b) lenses of the same size ($R_7 = 10\ \lambda_0$) illuminated by the CSP feed positioned at a certain distance from the lens surface. Solid and dashed lines are for E and H polarizations, respectively.

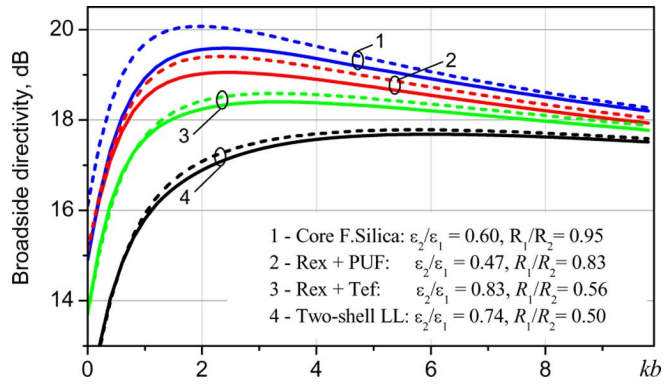

Fig. 10. Broadside directivity of the CSP assisted by two-shell lenses vs. beam waist parameter. Lenses have the same size ($R_2 = 10\ \lambda_0$) and the distance between the feed and the lens surface is $\delta = \lambda_0/10$. Solid and dashed lines are for E and H polarizations, respectively.

(2). As one can see, there exists an optimal value of the beam waist parameter that guarantees the best broadside directivity for the selected lens size and feed position (that is in line with earlier studies [16]). For the case of the CSP feed located close to the lens surface ($\delta = \lambda_0/10$), the optimal beam waist parameter value is $kb = 2.0$; it corresponds to a full half-power (-3 dB) beamwidth of 48°. It is interesting to note that this value does not depend on the lens size, although it is sensitive to the feed location (see Fig. 9(b)). The latter is due to the necessity of providing the same (optimal) edge illumination level of the lens aperture whose angular size decreases when the feed moves away from the lens surface.

For two-shell lenses these recommendations need to be refined depending on the lens structure. Fig. 10 represents broadside directivity of the CSP feed assisted by two-shell lenses considered in the communication. As seen, the smaller the relative core size of the lens, the larger kb value required to provide the best directivity. Note that larger kb value corresponds to narrower beam width, so this is a direct correlation between the core size and the optimal beam width.

In summary, according to Fig. 10, the average best value for the two-shell lenses is $kb = 3.0$ (that corresponds to the half-power beamwidth of 36° and the lens edge illumination level of about -8 dB). For convenience this value is used throughout the communication, although it might not be the best one for all the lens configurations studied (e.g., the best performance of the seven-shell LL and two-shell lenses with dense cores is achieved for $kb = 2.0$, whereas the optimal kb value for the Rex + Tef lens is 4.0).

REFERENCES

[1] T. L. A. Rhys, "The design of radially symmetric lenses," *IEEE Trans. Antennas Propag.*, vol. 18, no. 4, pp. 497–506, 1970.

[2] J. R. Sanford, "Scattering by spherically stratified microwave lens antennas," *IEEE Trans. Antennas Propag.*, vol. 42, no. 5, pp. 690–698, May 1994.

[3] B. Schoenlinner, X. Wu, J. P. Ebling, G. V. Eleftheriades, and G. M. Rebeiz, "Wide-scan spherical-lens antennas for automotive radars," *IEEE Trans. Microw. Theory Tech.*, vol. 50, no. 9, pp. 2166–2175, Sep. 2002.

[4] J. Thornton, "Wide-scanning multi-layer hemisphere lens antenna for Ka band," *IEE Proc. Microw. Antennas Propag.*, vol. 153, no. 6, pp. 573–578, Dec. 2006.

[5] B. Fuchs, L. L. Coq, O. Lafond, S. Rondineau, and M. Himdi, "Design optimization of multishell luneburg lenses," *IEEE Trans. Antennas Propag.*, vol. 55, no. 2, pp. 283–289, Feb. 2007.

[6] D. Gray, J. Thornton, and R. Suzuki, "Assessment of discretised sochacki lenses," in *Proc. Loughborough Antennas Propag. Conf. (LAPC)*, Nov. 2009, pp. 289–300.

[7] J. Thornton, A. White, and D. Gray, "Multi-beam lens-reflector for satellite communications: Construction issues and ground plane effects," in *Proc. 3rd Eur. Conf. Antennas Propag. (EuCAP)*, Berlin, Germany, 2009, pp. 1377–1380.

[8] T. Komljenovic, R. Sauleau, Z. Sipus, and L. L. Coq, "Layer circular-cylindrical dielectric lens antennas—Synthesis and height reduction technique," *IEEE Trans. Antennas Propag.*, vol. 58, no. 5, pp. 1783–1788, May 2010.

[9] A. M. Kapitonov and V. N. Astratov, "Observation of nanojet-induced modes with small propagation losses in chains of coupled spherical cavities," *Opt. Lett.*, vol. 32, pp. 409–411, Feb. 2007.

[10] N. A. Mortensen, O. Sigmund, and O. Breinbjerg, "Prospects for poor-man's cloaking with low-contrast all-dielectric optical elements," *J. Eur. Opt. Soc.*, vol. 4, 2009.

[11] R. K. Luneburg, *The Mathematical Theory of Optics*. Providence, RI: Brown Univ. Press, 1994.

[12] H. Mosallaei and Y. Rahmat-Samii, "Nonuniform Luneburg and two-shell lens antennas: Radiation characteristics and design optimization," *IEEE Trans. Antennas Propag.*, vol. 49, no. 1, pp. 60–69, Jan. 2001.

[13] K. Sato and H. Ujiie, "A plate Luneberg lens with the permittivity distribution controlled by hole density," *Electron. Commun. Jpn.*, vol. 85, no. 9, pt. Part 1, pp. 1–12, 2002.

[14] J. Kot, R. Donelson, N. Nikolic, D. Hayman, M. O'Shea, and G. Peeters, "A spherical lens for the SKA," *Exper. Astron.*, vol. 17, pp. 141–148, 2004.

[15] J. Kot, "A Luneburg Lens for the SKA: Summary of the MNRF Research Project into the Manufacture of a Low-Cost Microwave Refracting Spherical Lens for Radioastronomy," [Online]. Available: http://www.atnf.csiro.au/projects/mnrf2001/symposium2004/JSK.ppt

[16] A. V. Boriskin and A. I. Nosich, "Whispering-gallery and Luneburg-lens effects in a beam-fed circularly-layered dielectric cylinder," *IEEE Trans. Antennas Propag.*, vol. 50, no. 9, pp. 1245–1249, Sep. 2002.

[17] E. Heyman and L. B. Felson, "Gaussian beam and pulsed-beam dynamics: Complex-source and complex-spectrum formulations within and beyond paraxial asymptotics," *J. Opt. Soc. Am. A*, vol. 18, no. 7, pp. 1588–1611, 2001.

[18] G. L. Hower, R. G. Olsen, D. J. Earls, and J. B. Schneider, "Inaccuracies in numerical calculation of scattering near natural frequencies of penetrable objects," *IEEE Trans. Antennas Propag.*, vol. 41, no. 7, pp. 982–986, Jul. 1993.

[19] A. V. Boriskin, A. Rolland, R. Sauleau, and A. I. Nosich, "Test of the FDTD accuracy in the analysis of the scattering resonances associated with high-Q whispering-gallery modes of a circular cylinder," *J. Opt. Soc. Am. A*, vol. 25, no. 5, pp. 1169–1173, May 2008.

[20] A. Rolland, M. Ettorre, A. V. Boriskin, L. Le Coq, and R. Sauleau, "Axisymmetric resonant lens antenna with improved directivity in Ka-band," *IEEE Antennas Wireless Propag. Lett.*, vol. 10, no. 1, pp. 37–40, 2011.

[21] A. V. Boriskin, A. Vorobyov, and R. Sauleau, "Collimating and resonant properties of two-shell radially symmetric lenses," in *Proc. 5th Eur. Conf. Antennas Propag. (EuCAP)*, Rome, Italy, 2011, pp. 779–782.